EFFECTS OF HORIZONTAL AND VERTICAL NEAR-FAULT GROUND MOTIONS ON THE NONLINEAR DYNAMIC RESPONSE OF RC BUILDINGS WITH DIFFERENT BASE-ISOLATION SYSTEMS

F. Mazza[1] and A. Vulcano[2]

[1] *Researcher, Dept. of Engineering Modeling, University of Calabria, Rende (Cosenza), Italy*
[2] *Professor, Dept. of Engineering Modeling, University of Calabria, Rende (Cosenza), Italy*
Email: fabio.mazza@unical.it, vulcano@unical.it

ABSTRACT:

Near-fault ground motions are characterized by long-duration horizontal pulses and high peak values of vertical acceleration, which can become critical for a base-isolated structure. The objective of this work is to study effectiveness and limitations of base-isolation systems obtained considering High-Damping-Laminated-Rubber Bearings (HDLRBs) acting alone or either in parallel or in series with steel-PTFE sliding bearings. A numerical investigation is carried out with reference to base-isolated five-storey reinforced concrete buildings designed according to the European seismic code (Eurocode 8). The design of the base-isolated test structures (in case of HDLRBs only) is carried out in a high-risk seismic region considering the horizontal seismic loads acting in combination with the vertical ones and assuming different values of the ratio between horizontal stiffness and vertical stiffness of the HDLRBs. The behaviour of the frame members is simulated by a bilinear law, checking plastic conditions at potential critical sections. A viscoelastic model with variable stiffness properties in the horizontal and vertical directions, depending on the axial force and lateral deformation, simulates the response of a HDLRB. A rigid-plastic (with friction variability) law is assumed to simulate the behaviour of a steel-PTFE sliding bearing. The nonlinear dynamic behaviour of the test structures is studied under near-fault earthquakes.

KEYWORDS: base-isolated building, base isolation, elastomeric bearing, sliding bearing, nonlinear seismic analysis, near-fault earthquake

1. INTRODUCTION

In the last two decades the seismic isolation technique proved to be very effective for the seismic protection of new constructions as well as for the seismic retrofitting of existing ones. Design guidelines for seismically isolated structures have been developed in many countries with a high seismic hazard (ASSISi, 2003) and, lately, suitable code provisions have been drafted also in Europe (Eurocode 8, 2003: EC8).
The considerable horizontal deformability of a base-isolated structure may amplify the structural response under strong near-fault ground motions, which are characterized by long-duration horizontal pulses and so large displacements that an oversizing of the isolation system could be required (Kelly, 1999). Specifically, the frequency content of the motion transmitted by the isolators to the superstructure can become critical when the pulse intensity is so strong that the superstructure undergoes plastic deformations.
Strong near-fault ground motions are also characterized by high values of the ratio $\alpha_{PGA}(=PGA_V/PGA_H)$ between the peak value of the vertical acceleration, PGA_V, and the analogous value of the horizontal acceleration, PGA_H. High values of the acceleration ratio α_{PGA} can notably modify the axial load in reinforced concrete (r.c.) columns, producing undesirable phenomena (Papazoglou and Elnashai, 1996): e.g., buckling of the longitudinal bars, brittle failure in compression, bond deterioration or failure under tension. In addition, plastic hinges are expected along the span of the girders owing to the vertical acceleration, especially at the upper storeys, where the effects of the gravity loads generally prevail over those of the horizontal seismic loads and an amplification of the vertical motion is expected also depending on the vertical stiffness of the isolators (Mazza and Vulcano, 2006a, 2006b).
To overcome the above problems, many solutions using different isolation systems were proposed (e.g., Jangid and Kelly, 2001, Mazza and Vulcano, 2004). The objective of this work is to compare different base-isolation techniques, evaluating their effects and applicability limits through the study of the nonlinear dynamic response of base-isolated five-storey r.c. framed buildings subjected to horizontal and vertical near-fault ground motions.

2. LAYOUT AND MODELING OF THE BASE ISOLATION SYSTEMS

Base isolation systems are usually realized by elastomeric bearings (filtering the horizontal ground motion so that its predominant periods are longer than the vibration periods characterizing the response of the superstructure) and frictional-bearings (limiting the maximum acceleration transmitted to the superstructure).
The response of a High-Damping-Laminated-Rubber (HDLR) bearing under a lateral loading (F), acting simultaneously with a compressive or tensile axial loading (P), exhibits a horizontal displacement (u_H) and a vertical displacement ($\pm u_V$). Experimental results available in literature pointed out that the horizontal stiffness, K_H, decreases (starting from the nominal value, K_{H0}) under increasing vertical load (Naeim and Kelly, 1999), while the corresponding vertical stiffness, K_V, decreases (starting from the nominal value, K_{V0}) for increasing lateral deformation (Ryan *et al.*, 2004). A two-spring-two-dashpot model, with a nonlinear spring acting in parallel with a linear viscous dashpot both along the horizontal and vertical directions, can be adopted for modeling a HDLR bearing (Fig. 1a). To simulate the observed behaviour, the nonlinear force-displacement laws for the horizontal spring (F_K-u_H) and the vertical one (P_K-u_V) are expressed as

$$F_K = K_H u_H = K_{H0}\left[1-\left(\frac{P}{P_{cr}}\right)^2\right]u_H \quad ; \quad P_K = \left[K_{V0}\left(u_V - \frac{\alpha_b}{\alpha_{K0}}\frac{16}{\pi^2\phi_b S_2}u_H^2\right)\right] \Big/ \left[1+48\left(\frac{u_H}{\pi\phi_b}\right)^2\right] \qquad (2.1a,b)$$

where: P_{cr} is the compressive or tensile critical load (Naeim and Kelly, 1999); ϕ_b is the diameter of the bearing (circular section); $\alpha_b=h_b/t_r$, being h_b and t_r the total height of the bearing and rubber, respectively (e.g., $\alpha_b=1.2$ can be considered as a mean value); $\alpha_{K0}(=K_{V0}/K_{H0})$ is the nominal stiffness ratio of the isolator (e.g., $\alpha_{K0}=800$ can be considered as a typical value); $S_2=\phi_b/t_r$ is the secondary shape factor. As proposed by Naeim and Kelly (1999), it is possible to obtain fairly accurate information on the stability of a bearing in the deformed configuration adopting the expression of the compressive or tensile critical load (P_{cr}) calculated in the undeformed configuration, but replacing the cross-sectional area (A) with the reduced effective area (i.e., the area of overlap between the top and bottom of the isolator, A_r), function of the lateral displacement:

$$P_{cr} = \left(\pi G S_1 S_2 \sqrt{A A_r}\right) \Big/ \left(2\sqrt{2}\right) \qquad (2.2)$$

where G is the shear modulus and $S_1(=\phi_b/(4t)$, being t the thickness of the single layer of rubber) is the primary shape factor.
Furthermore, the linear force-velocity laws for the horizontal dashpot (F_C-$\dot{u}_H$) and the vertical one (P_C-$\dot{u}_V$) can be expressed as (Mazza and Vulcano, 2007)

$$F_C = C_H \dot{u}_H \cong \xi_H K_H T_{1H} \dot{u}_H / \pi \quad ; \quad P_C = C_V \dot{u}_V \cong \xi_V K_V T_{1V} \dot{u}_V / \pi \qquad (2.3a,b)$$

where ξ_H (ξ_V) and T_{1H} (T_{1V}) represent, respectively, the equivalent viscous damping ratio and the fundamental vibration period in the horizontal (vertical) direction.
The response of a steel-PTFE sliding bearing, under a lateral loading acting simultaneously with a compressive axial loading (P), basically depends on sliding velocity, contact pressure and temperature (Dolce *et al.*, 2005; Mokha *et al.*, 1990). More specifically, the coefficient of sliding friction increases with increasing velocity up to a certain velocity value, beyond which it remains almost constant, while drops with increasing pressure - with a rate of reduction that is dependent on sliding velocity - and temperature. The frictional force at the sliding interface can be expressed as (Constantinou *et al.*, 1990)

$$F_F = \mu_F \cdot P \cdot Z \quad ; \quad \mu_F = \mu_{max} - (\mu_{max} - \mu_{min}) \cdot e^{-\alpha \dot{u}_H} \qquad (2.4a,b)$$

where Z is a dimensionless hysteretic quantity (Z takes values of ± 1 during sliding and less then unity during sticking) and μ_F is the coefficient of friction at sliding velocity $\dot{u}_H$, which attains the value μ_{max} or μ_{min} respectively at high or very low velocity, while α is a constant for given values of pressure and temperature.
The large horizontal base displacement consequent to a near-fault ground motion can be enabled by oversizing the elastomeric bearings (e.g., increasing the geometric dimensions of the rubber layers) or the frictional bearing (e.g., increasing the roughness of the sliding surface). In alternative, the elastomeric bearing may act in parallel with a sliding bearing (e.g., the "Resilient-Friction Base Isolator", R-FBI) or in series with a sliding plate (e.g., the *Electricité de France* system, EDF) attached to its top or bottom surface and placed against a metal plate (Naeim and Kelly, 1999). However, the Base Isolation with in-Parallel Sliding (BIPS) system presents the

problem of increasing the contribution of the higher vibration modes of the superstructure, while the Base Isolation with in-Series Sliding (BISS) system is not always favourable in reducing the residual displacement of the isolation system. The behaviour of the base-isolation systems illustrated above can be simulated by adopting the models shown in Fig. 1. More specifically, Figs. 1a and 1b refer, respectively, to elastomeric and frictional bearings, while Figs. 1c and 1d represent, respectively, BIPS and BISS systems. It is worth to mention that models and constitutive laws more sophisticated can be found in literature, but the relatively simple assumptions above considered are preferable to carry out nonlinear dynamic analysis with a reasonable computational effort.

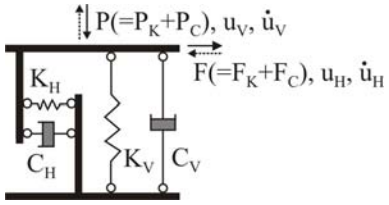

(a) Elastomeric bearing (e.g., HDLR bearing)

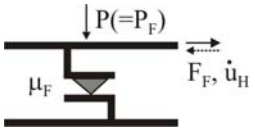

(b) Frictional bearing (e.g., steel-PTFE bearing)

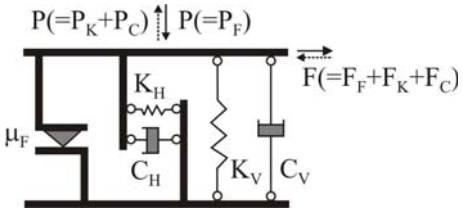

(c) In-parallel combination of elastomeric and sliding bearings (BIPS system: e.g., R-FBI)

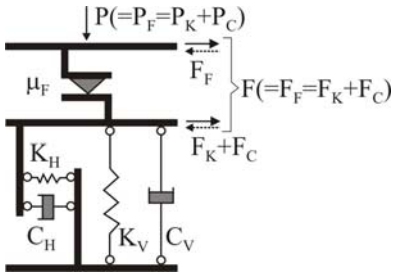

(d) In-series combination of elastomeric bearing and sliding plates (BISS system: e.g., EDF)

Figure 1 Modeling of base-isolation systems

3. LAYOUT AND DESIGN OF THE BASE-ISOLATED TEST STRUCTURES

A typical five-storey residential building, with a reinforced concrete (r.c.) framed structure isolated at the base by HDLR bearings, is considered as a reference for the numerical investigation (Fig. 2a). Because of the structural symmetry and assuming the floor slabs infinitely rigid in their own plane, the entire structure is idealized by an equivalent plane frame (BI: Fig. 2b), whose elements have stiffness and strength properties so that the perimeter frames and the interior ones (placed along the horizontal motion direction) could be represented as a whole (in the hypothesis that the three interior frames have the same properties), assuming the tributary mass resulting from the overall building and the gravity loads corresponding (for a perimeter frame or an interior one) to the tributary area marked in Fig. 2a. Infill walls, placed along the perimeter of the building, are assumed as non-structural elements regularly distributed in elevation. A grid of rigid girders is assumed placed, at the base of the framed structure, on the HDLR bearings. Geometric dimensions of the test frame and size of the sections, for girders and columns of each storey, are also shown in Fig. 2b. In order to take into account the plastic deformations along the girders, each of these is discretized into four sub-elements of equal length; in this way, the potential critical sections correspond to end, quarter-span and mid-span sections (Fig. 2b). Further detail can be found in a previous work by the authors (Mazza and Vulcano, 2007).

The proportioning of the test structures was done according to EC8 assuming, besides the gravity loads, the horizontal and vertical seismic loads. Moreover, the following assumptions are made: elastic response of the superstructure (behaviour factor for the horizontal seismic loads, q_H=1; behaviour factor for the vertical seismic loads, q_V=1); moderately soft soil (subsoil class D); high risk seismic region (PGA_H=0.47g; PGA_V=0.315g). The gravity loads used in the design are represented by dead- and live-loads, respectively equal to: 4.3 kN/m^2 and 1 kN/m^2, for the top floor; 5 kN/m^2 and 2 kN/m^2, for the other floors. The contribution of the perimeter masonry-infills is taken into account considering a weight of 2.7 kN/m^2. A cylindrical compressive strength of 30 N/mm^2 for concrete and a yield strength of 375 N/mm^2 for steel are assumed for the r.c. frame members. At each floor of a BI structure (Fig. 2b), the following masses are considered: lumped masses at the exterior and interior joints, in order to take into account the contribution of the transverse girders and, in case of the exterior

joints, also the one of the masonry infills; uniformly distributed mass along the girders and columns, accounting for the gravity load of the structural member and, in the case of a girder, also of the floor slab and masonry infills (only for girders of perimeter frames). Specifically, at the level of the rigid girders placed on the HDLR bearings, lumped and distributed masses are assumed 1.5 times the ones at the first floor. It is worth mentioning that the same cross-sectional area is assumed for the exterior isolators and the interior ones of both perimeter and interior frames. Three cases are examined, referring to the fundamental vibration period in the horizontal direction T_{1H}=2.5 s, assumed as a reference value, and to three values of fundamental vibration period in the vertical direction (i.e., T_{1V}=0.186 s, 0.121 s and 0.106 s) corresponding to three values of the nominal stiffness ratio of an isolator (i.e., α_{K0}= 200, 800, 2000).

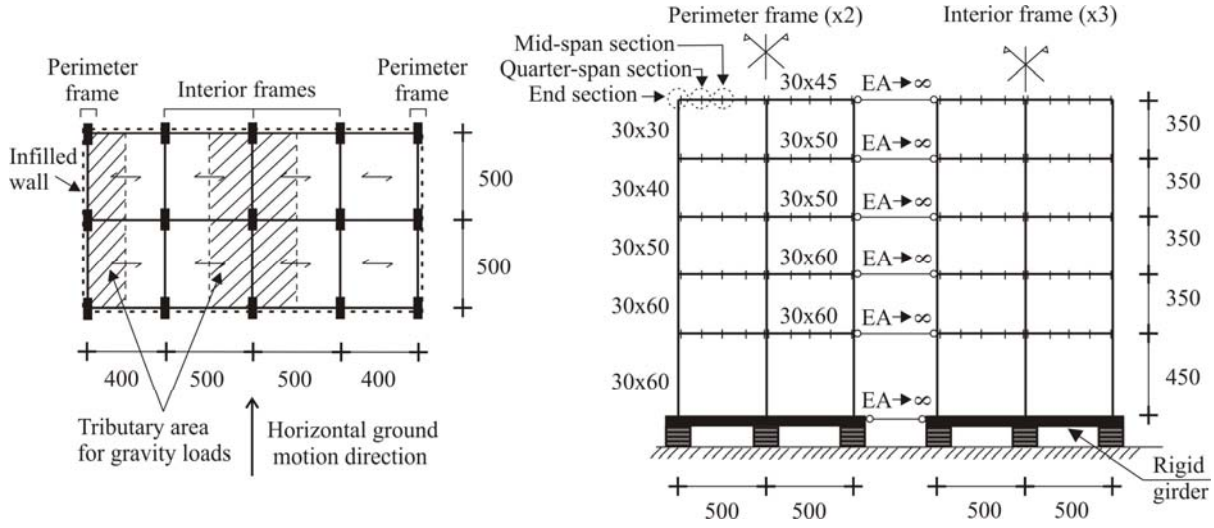

(a) Plan of the framed building structure (b) Plane structure (BI) equivalent to the spatial one

Figure 2 Base-isolated r.c. test structure (dimensions in cm)

The design is carried out considering the maximum value of the stresses obtained combining the horizontal (or vertical) seismic loads with 30% of the vertical (or horizontal) seismic loads. With regard to the design of the superstructure, in the three examined cases (see three values of α_{K0}), minimum conditions for the longitudinal bars of the girders and columns, according to the prescriptions for low ductility class imposed by EC8, are satisfied. The design of the HDLR bearings is carried out according to the prescriptions imposed by EC8, assuming a shear modulus of the elastomer G=0.35 MPa. In Table 3.1, for each value of α_{K0} considered in the analysis, the following data are reported: diameter of the bearings (ϕ_b); primary shape factor (S_1) and secondary shape factor (S_2); compression modulus (E_c), which is calculated according to EC8 as depending on G, S_1 and volumetric compression modulus of the rubber (E_b). The HDLR bearings fulfill the ultimate limit state (ULS) verifications regarding the maximum shear strains: i.e., $\gamma_{tot}=\gamma_s+\gamma_c+\gamma_\alpha\leq 5$ and $\gamma_s\leq 2$, where γ_{tot} represents the total design shear strain, while γ_s, γ_c and γ_α represent the shear strain of the elastomer owing to seismic displacement, axial compression and angular rotation, respectively. Moreover, the maximum compression axial load (P) does not exceed the critical load (P_{cr}) divided by a safety coefficient equal to 2 (i.e., $P_{cr}/P_c\geq 2$). Finally, the maximum value of the tensile stress (σ_t) resulting from the seismic analysis is assumed as 2G(=0.7 MPa) for all the isolators. In Table 3.1 the results of the above ULS verifications for the isolators are also reported. As can be observed, the design of the isolators has been generally limited by the condition imposed on the maximum shear strains (i.e., γ_{tot} and γ_s), with the exception of α_{K0}=200 where the buckling control proved to be the more restrictive. Finally, no tensile forces were found in the isolators.

Table 3.1 Geometrical and mechanical properties of the HDLR bearings

α_{K0}	ϕ_b (mm)	S_1	S_2	E_c (MPa)	γ_s	γ_{tot}	$(P_{cr}/P_c)_{min}$
200	1007	5.71	2.66	66	0.90	3.85	2.00
800	733	12.60	3.48	273	1.64	5.00	2.70
2000	657	24.81	3.78	694	2.00	4.46	4.55

4. NUMERICAL RESULTS

In order to evaluate the effects produced by the combination of the horizontal and vertical components of near-fault ground motions on the response of base-isolated r.c. framed buildings, a numerical investigation is carried out. The nonlinear analysis of the test structures is carried out by using a step-by-step procedure, which is based on a two-parameter implicit integration scheme and an initial-stress-like iterative procedure (Mazza and Vulcano, 2006a,b). At each step of the analysis, plastic conditions are checked at the potential critical sections of the girders and columns. A bilinear beam model is adopted, assuming a hardening ratio of 5% and fully elastic axial strains; the effect of the axial load on the ultimate bending moment of the columns (M-N interaction) is also considered. A viscoelastic model with variable stiffness properties in the horizontal and vertical directions, depending on the axial force and lateral deformation, simulates the response of a HDLR bearing (see Eqs. 2.1, 2.2, 2.3), while a rigid-plastic law with friction variability (see Eqs. 2.4a,b) is assumed to simulate the behaviour of a steel-PTFE sliding bearing.

Specifically, the nonlinear dynamic response of BI structures, described in Section 3 with reference to three values of the nominal stiffness ratio of the isolators (i.e., α_{K0}=200, 800, 2000), is studied under Taiwan (Chi-Chi TCU068 station: E-W and vertical components) and Imperial Valley (El Centro D.A. station: horizontal, 360, and vertical components) earthquakes. The results obtained for BI structures are compared with those for cases in which the HDLR bearings are combined with: (a) in parallel steel-PTFE sliding bearings (Fig. 1c: BIPS system); (b) in series steel-PTFE sliding plates (Fig. 1d: BISS system). In Fig. 4 arrangements of the elastomeric and sliding bearings (or plates) considered in the present work are schematically shown. Each arrangement corresponds to a value of the sliding ratio α_S(=$F_S/F_{S,max}$), defined, under gravity loads, as the global sliding force (F_S) corresponding to an examined BIPS (Fig. 4a) or BISS (Fig. 4b) system divided by the maximum sliding force ($F_{S,max}$), this last one evaluated supposing that elastomeric and sliding bearings (or plates) are placed under each column. More precisely, three cases are considered (i.e., α_S=1/4, 1/2, 3/4) evaluating the sliding friction coefficient μ_F (see Eq. 2.4b) for mean values of contact pressure and temperature, e.g. assuming (see Dolce *et al.*, 2005): μ_{min}=5%, μ_{max}=15% and α=0.02 s/mm.

First, the response of BI, BIPS and BISS structures is studied under Chi-Chi (duration: 35s) and Imperial Valley (duration: 20s) ground motions. To this aim, in Table 4.1 the time (t) in which the analysis is stopped and the corresponding limit state which is reached are reported for all the examined cases. Specifically, the ultimate values of the total shear strain ($\gamma_{tot,u}$) and the corresponding shear strain owing to seismic displacement ($\gamma_{s,u}$) of a HDLR bearing are assumed equal to 7.5(=1.5×5) and 3(=1.5×2), respectively; moreover, the compressive and tensile axial loads are limited, respectively, to the critical buckling load (P_{cr}), evaluated according to Eq. 2.2, and the tensile value (P_{tu}), obtained multiplying the reduced effective area by a limit stress tension (σ_{tu}) equal to 0.7 MPa. Finally, no tensile axial load (i.e., σ_{tu}=0) is accepted for steel-PTFE sliding bearings (plates) in the cases of BIPS and BISS systems. As can be observed, the analyses of BI and BISS structures were stopped once $\gamma_{tot,u}$ or σ_{tu} was reached. This occurred, under both Chi-Chi earthquake (with the exception of BI structure, in the case of α_{K0}=200), characterized by high values of the spectral acceleration in the horizontal direction, and Imperial Valley earthquake (with the exception of BI structures, in the cases of α_{K0}=200 and α_{K0}=800, and BISS structures, for α_{K0}=200), characterized by high values of the spectral acceleration in the vertical direction (for spectra see Mazza and Vulcano, 2007). On the other hand, the analyses of the BIPS structures were stopped, in all the examined cases, at different times, because, as assumed above, tensile forces are not accepted.

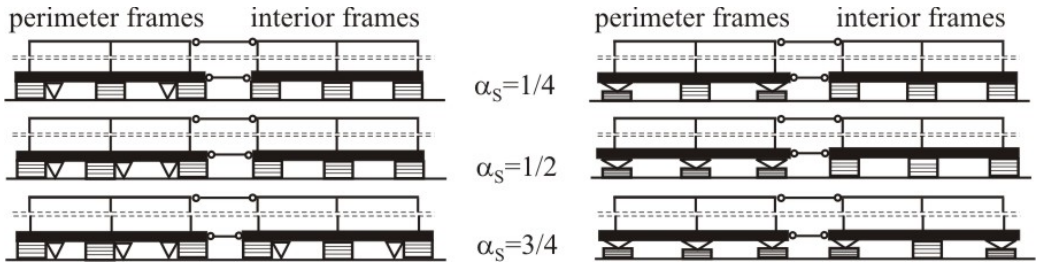

(a) BIPS systems (b) BISS systems

Figure 4 Arrangements of HDLR bearings with in-parallel (a) and in-series (b) sliding system

Table 4.1 Response parameters for BI, BIPS and BISS systems under Chi-Chi and Imperial Valley earthquakes

		Chi-Chi (TCU068: E-W+Vert.)			*Imperial Valley (El Centro D.A.: 360 + Vert.)*		
α_{K0}	α_s	*BI*	*BIPS*	*BISS*	*BI*	*BIPS*	*BISS*
200	0	t=35 s	-	-	t=20 s	-	-
	1/4	-	t=12.23 s σ_{tu}=0	t=12.13 s $\gamma_{tot,u}$=7.5	-	t=3.63 s σ_{tu}=0	t=20 s
	1/2	-	t=10.72 s σ_{tu}=0	t=12.10 s $\gamma_{tot,u}$=7.5	-	t=3.61 s σ_{tu}=0	t=20 s
	3/4	-	t=10.71 s σ_{tu}=0	t=12.32 s $\gamma_{tot,u}$=7.5	-	t=3.61 s σ_{tu}=0	t=20 s
800	0	t=11.94 s; γ_{tot}=7.5	-	-	t=20 s	-	-
	1/4	-	t=10.77 s σ_{tu}=0	t=11.93 s $\gamma_{tot,u}$=7.5	-	t=3.35 s σ_{tu}=0	t=3.47 s σ_{tu}=0
	1/2	-	t=10.71 s σ_{tu}=0	t=11.94 s $\gamma_{tot,u}$=7.5	-	t=3.47 s σ_{tu}=0	t=3.47 s σ_{tu}=0
	3/4	-	t= 0.70 s σ_{tu}=0	t=12.08 s $\gamma_{tot,u}$=7.5	-	t=3.35 s σ_{tu}=0	t=3.47 s σ_{tu}=0
2000	0	t=11.95 s; γ_{tot}=7.5	-	-	t=3.54 s; σ_{tu}=0.7 MPa	-	-
	1/4	-	t=11.98 s σ_{tu}=0	t=11.93 s $\gamma_{tot,u}$=7.5	-	t=3.53 s σ_{tu}=0	t=3.54 s σ_{tu}=0
	1/2	-	t=10.71 s σ_{tu}=0	t=11.94 s $\gamma_{tot,u}$=7.5	-	t=3.54 s σ_{tu}=0	t=3.54 s σ_{tu}=0
	3/4	-	t=10.70 s σ_{tu}=0	t=12.06 s $\gamma_{tot,u}$=7.5	-	t=3.53 s σ_{tu}=0	t=3.54 s σ_{tu}=0

Successively, the effectiveness of the BIPS and BISS systems in order to control the displacement undergone by the base-isolation system has been investigated. To this aim, time histories of the maximum isolator horizontal displacement are plotted in Fig. 5, assuming different values of the sliding ratio (i.e., α_s=0, 1/4, 1/2, 3/4). More specifically, the results have been obtained with reference to the horizontal (E-W) and vertical components of the Chi-Chi earthquake, assuming a stiffness ratio of the rubber bearings α_{K0}=800. As can be observed, the in-parallel insertion of sliding bearings (Fig. 5a) has been always favourable to control the isolators' displacement: the choice of increasing the α_S value produces the reduction of the isolator displacement. However, the use of the BIPS system can need re-centring after an earthquake, in case the elastic restoring force produced by the elastomeric isolators does not exceed the friction threshold imposed by the sliding bearings. The in-series addition of sliding plates (Fig. 5b) does not correspond always to a reduction of the maximum horizontal displacement of the base-isolation system: indeed, the curves for different values of α_S are comparable. Moreover, the re-centring of the BISS system may present some difficulty when the residual displacement is a combination of out-of-phase movements of an isolator and the corresponding sliding plates.

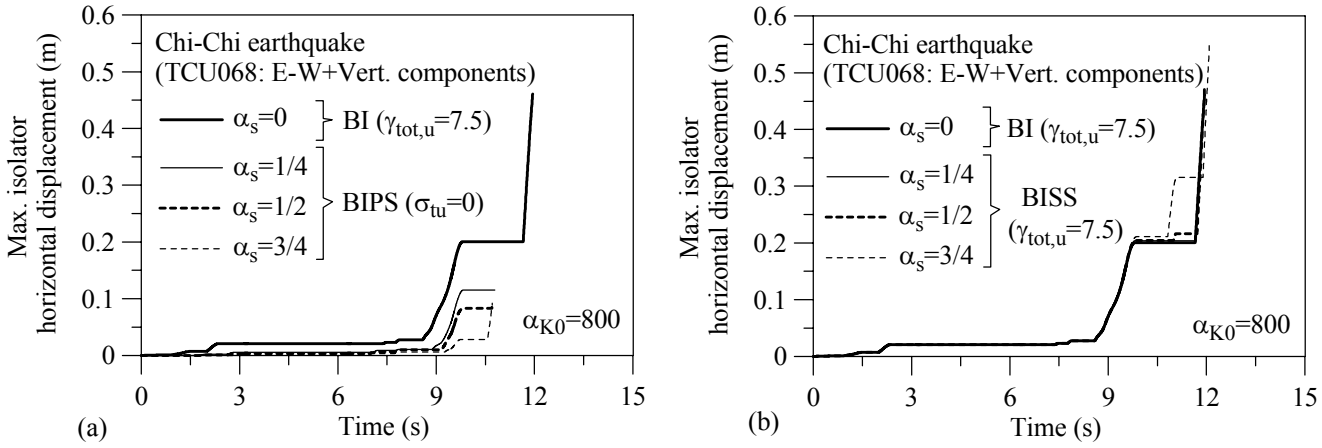

Figure 5 Time histories of the maximum isolator horizontal displacement for different values of the sliding ratio α_S

To check the effectiveness of sliding bearings (or plates) for controlling the damage at potential critical sections of the girders and columns, time histories of the maximum value of the curvature ductility demand attained at the critical sections of r.c. frame members are plotted in Fig. 6. More precisely, curves obtained for BIPS and BISS systems, assuming different values of the sliding ratio α_S and a stiffness ratio α_{K0}=800, are plotted for the Chi-Chi earthquake. The results show that the BIPS system (Fig. 6a) does not improve the performance of the superstructure; the performance gets even worse of that observed for the BI structure, especially for increasing values of α_S, because the structural behaviour becomes ever-closer to that of a fixed-base structure. It is useful to note that, as already observed by Mazza and Vulcano, 2007, the pulse-type E-W component of Chi-Chi earthquake induces ductility demands at the end sections of both girders and columns, especially at the lower storeys. On the other hand, the BISS system (Fig. 6b) proves to be generally effective for controlling the structural damage of the framed structure, producing elongation of the effective fundamental vibration period, thus limiting the maximum horizontal acceleration transmitted to the superstructure.
Finally, in Fig. 7 time histories of the maximum ductility demand at critical sections of the r.c. frame members of structures with BIPS (Fig. 7a) and BISS (Fig.7b) systems subjected to Imperial Valley earthquake are plotted, assuming α_s=1/2 and different values of stiffness ratio (α_{K0}=200, 800, 2000). Also in this case, the adoption of the BISS system allows, for each α_{K0} value, improvement of the structural performance in comparison with that for the BIPS system. Specifically, the BISS system leads to a basically elastic behaviour of the superstructure, at least for a rather low value of α_{K0} (e.g., α_{K0}=200), for which the structure behaves as isolated also along the vertical direction. However, it has been observed that the BIPS system produces high ductility demand, especially at the end and mid-span sections of the girders placed at the top floor of the perimeter frames; in addition, for a rather high α_{K0} value (e.g., α_{K0}=2000), for which the superstructure behaves as a fixed-base one in the vertical direction, also girders at top floor of the interior frames underwent plastic deformations.

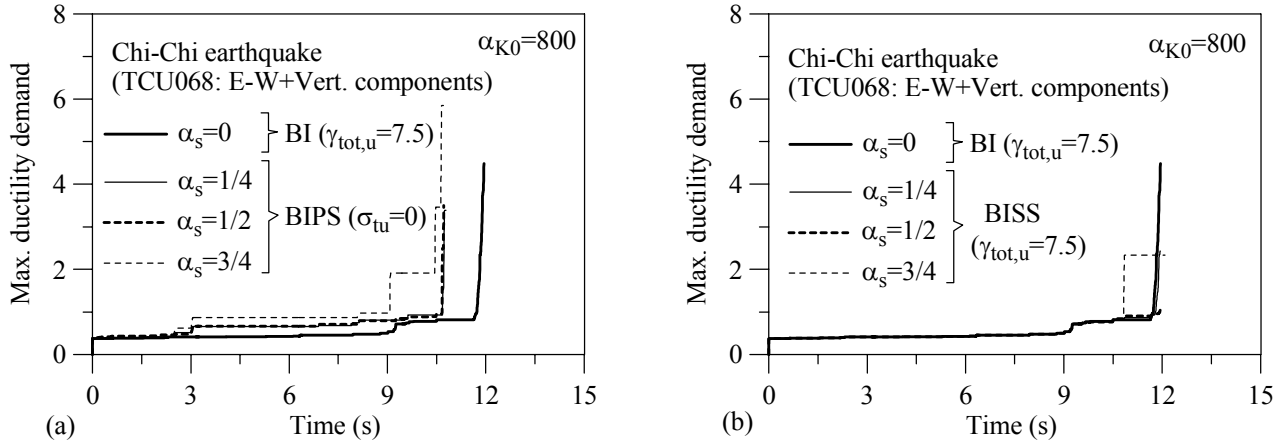

Figure 6 Time histories of the maximum ductility demand at r.c. member sections for different values of sliding ratio α_S

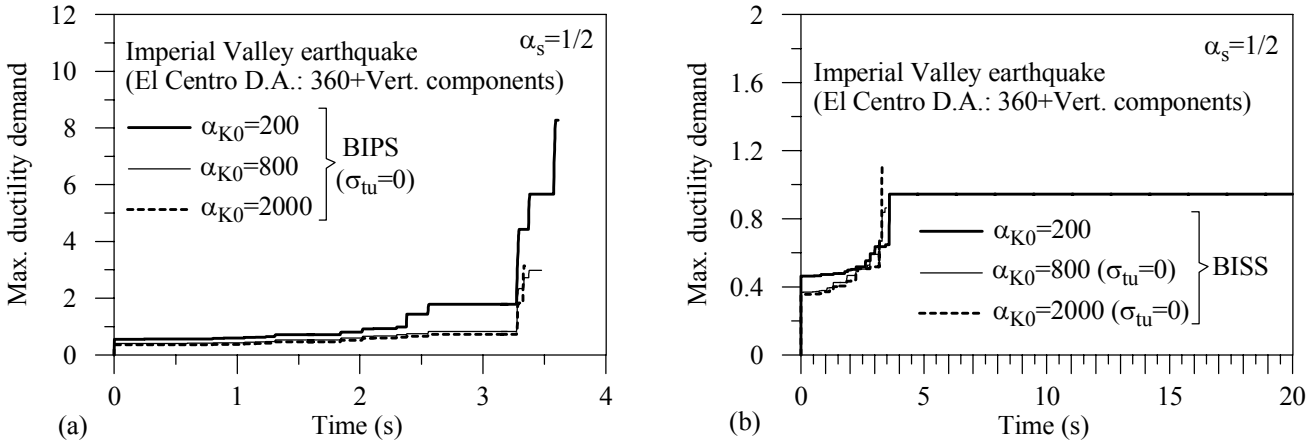

Figure 7 Time histories of the maximum ductility demand at r.c. member sections for different values of stiffness ratio α_{K0}

5. CONCLUSIONS

The nonlinear response of five-storey r.c. framed buildings with different base-isolation systems has been studied under near-fault ground motions. The following conclusions can be drawn from the results.
Unlike a BISS system, a BIPS one is effective for controlling the horizontal displacement of isolators. Both systems may need re-centring after an earthquake, but some difficulty may arise for out-of-phase movements of isolator and sliding plates of a BISS system. The adoption of a BISS system proves effective for controlling the damage of r.c frame members, producing an elongation of the effective fundamental vibration period in comparison with that of the BI structure; moreover, for a rather low α_{K0} value, the superstructure behaves as isolated in vertical direction. On the other hand, the adoption of a BIPS system, under a pulse-type horizontal component of a near-fault motion, can induce larger damage at end sections of both girders and columns, especially at the lower storeys; moreover, for a rather high α_{K0} value, the superstructure behaves as fixed-base in vertical direction and larger damage is undergone at end and mid-span sections of girders at the top floor.

ACKNOWLEDGMENTS

The present work was financed by R.E.L.U.I.S. (Italian network of university laboratories of earthquake engineering), according to “convention D.P.C. – R.E.L.U.I.S. 11/07/2005 (item 540) research line no. 7”.

REFERENCES

ASSISi (2003). Design rules and guidelines for structures provided with passive control systems of seismic vibrations applied or proposed in Armenia, Chile, France, Italy, Japan, Mexico, P. R. China, Russian Federation, U.S.A.. *Technical Report No. A/03-01, ENEA ed. for ASSISi*, Bologna, Italy.

Constantinou, M., Mokha, A. and Reinhorn, A. (1990). Teflon bearings in base isolation. II: modeling. *Journal of Structural Engineering*, 116(2): 455-474.

Dolce, M., Cardone, D. and Croatto, F. (2005). Frictional behaviour of steel-PTFE interfaces for seismic isolation. *Bulletin of Earthquake Engineering*, 3: 75-99.

Eurocode 8 (2003). *Design* of structures for earthquake resistance - part 1: general rules, seismic actions and rules for buildings. *C.E.N., European Committee for Standardization.*

Jangid, R.S. and Kelly, J.M. (2001). Base isolation for near-fault motions. *Earthquake Engineering and Structural Dynamics*, 30: 691-707.

Kelly, J.M. (1999). The role of damping in seismic isolation. *Earthquake Engineering and Structural Dynamics*, 28: 1717-1720.

Mazza, F. and Vulcano, A. (2004). Base-isolation techniques for the seismic protection of rc framed structures subjected to near-fault ground motions. *Procs. 13th World Conference on Earthquake Engineering,* Vancouver, Canada, paper 2935.

Mazza, F. and Vulcano, A. (2006a). Seismic response of base-isolated buildings under horizontal and vertical near-fault ground motions. *Procs. 8th U.S. National Conference on Earthquake Engineering, 100th Anniversary Earthquake Conference Commemorating the 1906 San Francisco Earthquake,* paper 485.

Mazza, F. and Vulcano, A. (2006b). Nonlinear response of base-isolated buildings under near-fault ground motions. *Procs. 1st European Conference on Earthquake Engineering and Seismology,* Geneva, Switzerland, paper 481.

Mazza, F. and Vulcano, A. (2007). Nonlinear dynamic response of r.c. base-isolated framed structures subjected to near-fault ground motions (in Italian). *Procs. XII Convegno L’Ingegneria Sismica in Italia, ANIDIS (Italian Association of Earthquake Engineering),* Pisa, Italy, paper 218.

Mokha, A., Constantinou, M. and Reinhorn, A. (1990). Teflon bearings in base isolation. I: testing. *Journal of Structural Engineering* 116(2): 438-454.

Naeim, F. and Kelly, J.M. (1999). Design of seismic isolated structures: from theory to practice. *John Wiley & Sons Ltd,* New York, U.S.A..

Papazoglou, A.J. and Elnashai, A.S. (1996). Analytical and field evidence of the damaging effect of vertical earthquake ground motion. *Earthquake Engineering and Structural Dynamics*, 25: 1109-1137.

Ryan, K.L., Kelly J.M. and Chopra, A.K. (2004). Experimental observation of axial load effects in isolation bearings. *Procs. 13th World Conference on Earthquake Engineering,* Vancouver, Canada, paper 1707.